

DIRECT AND INDIRECT EFFECTS OF URBAN POLLUTION AND LAND-USE CHANGE IMPACTS: A COMPARISON

Gustavo G. Carrió and William R. Cotton

Department of Atmospheric Science, Colorado State University, Fort Collins, Colorado

1. INTRODUCTION

Houston is one of the fastest growing metropolitan areas in the United States during the past three decades. The effects of growth of the Houston Metropolitan Area on the characteristics and intensity of convection and precipitation were investigated using the Regional Atmospheric Modeling System developed at Colorado State University (RAMS@CSU) coupled to the Town Energy Budget (TEB) urban model.

Our studies focused on events triggered by the sea-breeze circulation and were performed in four phases that used an identical modeling framework. The first phase (Carrió et al, 2010) focused on the land-use change effects. This first series of simulations used a case study (August 24, 2000) as a benchmark and the 1992, 2001, 2006 high-resolution National Land Cover Data (NLCD) for an objective experimental design. The second phase examined the indirect effects of urban pollution considering sources of varied intensity linked to sub-grid urban area fractions. The dependence of the intensification of the convective cells downwind of the city due to urban pollution indirect effects on the convective instability was analyzed in a third phase (Carrió and Cotton 2011). Finally, the fourth series of simulations focused on the direct (radiative) impact of urban pollution on precipitation and convection, and on the comparison of the various aforementioned effects.

In summary, our results indicate that changes in land-surface properties associated with growth of the urban complex and its interaction with the sea-breeze circulation are the dominant effect. The invigoration of downwind convective cells is caused by the additional latent heat release linked to an enhancement of supercooled liquid production in polluted aerosol plumes. This effect ranks second to land-use changes in importance and mainly affects the intensity and precipitation of individual downwind cells without modifying significantly integral precipitation values.

Finally, the direct radiative effects of pollution generate a surface cooling and a non-negligible reduction of convective instability and precipitation. However, the later ranks third in importance, especially over the area downwind of the city.

2. THE ATMOSPHERIC MODEL

For these series of numerical experiments, we implemented the Town Energy Budget (TEB) urban model into the Regional Atmospheric Modeling System developed at Colorado State University (RAMS@CSU, Cotton et al., 2003). The urban model TEB is now coupled to run in parallel as to maximize the full potential of our computing resources.

The Landsat Thematic Mapper™ National Land Cover Data (NLCD) for the Houston area corresponding to the years 1992, 2001, and 2006 were used as benchmarks for the experimental design of the land-use sensitivity experiments, including a run with "no city".

RAMS@CSU was configured to use three two-way interactive nested model grids with 42 vertical levels and horizontal grid spacings of 15.0, 3.75, and 0.75 km centered over Houston. Grid 1 (71X61 grid points) and Grid 2 (102X102 grid points) were used to simulate the synoptic and mesoscale environments, respectively. While Grid 3 (202X202 grid points) was used to resolve deep convection as well as the sea breeze circulation. Figure 1 gives the grid configuration used for these series of sensitivity experiments..

The microphysical modules consider the explicit activation of CCN (and giant CCN), a bimodal representation of cloud droplets, a bin-emulating approach for droplet collection, ice-particle riming, and sedimentation (Saleeby and Cotton, 2004, 2998). In addition, the radiative transfer modules take into account the direct (radiative) effects of urban particulate pollution.

The mixing ratios and number concentrations of all water species (cloud droplets, drizzle drops, rain, pristine ice crystals, snow crystals, aggregates, graupel and hail) were predicted. CCN, giant CCN and ice forming nuclei (IFN) concentrations were also considered as prognostic variables.

* *Corresponding author address:* Gustavo Gabriel Carrió, Department of Atmospheric Science, Colorado State University, Fort Collins, CO 80523; email: carrio@atmos.colostate.edu

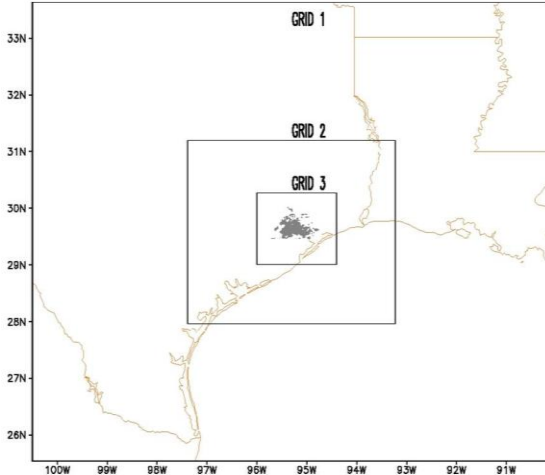


Figure 1: Grids 1, 2 and 3 used for all sensitivity experiments. The shaded area indicates the location of Houston.

3. EXPERIMENTAL DESIGN

3.1 Land-use sensitivity experiments.

The high-resolution NLCD satellite data for the Houston area corresponding to the years 1992, 2001, and 2006 were used as benchmarks for the experimental design of the land-use sensitivity experiments. One of the numerical experiments used the satellite data closest to the case we used for this study (2001), although, the urban cells were replaced by the predominant land use categories in the city surroundings (NO CITY).

3.2 Indirect aerosol effects

We also considered a series of numerical experiments varying the intensity of CCN sources linked to the urban area (no sensitivity runs have been performed varying giant CCN). To choose CCN concentrations representative of a highly polluted day, we analyzed two aerosol data sets documented during the Texas Air Quality Study / Gulf of Mexico Atmospheric Composition and Climate Study (TexAQS-GoMACCS; Lance et al, 2009). Athanasios Nenes and Patricia Quinn provided CCN measurements on the CIRPAS Twin Otter and NOAA P-3 and the data collected by the Ronald H. Brown ship. These 1-min temporal series of condensation nuclei (CN) concentrations, CCN/CN ratios, and the corresponding supersaturations were processed for the entire period to make the concentrations consistent with what "CCN" means for the activation routine in RAMS@CSU (i.e., the haze

particles or maximum concentration of cloud droplets that can be activated). Peak CCN concentrations exceeded 25000 cm^{-3} ; however, we eventually used lower CCN concentrations. A series of preliminary tests indicated that increasing the latter above 4000 cm^{-3} did not produce a significant impact on the results. City CCN sources were considered by nudging high concentrations (1000, 2000, 3000, and 4000 cm^{-3}) at the first model level above the ground multiplied by the sub-grid urban fraction of the corresponding grid cell. In addition to high CCN concentrations over the city, we initialized the surroundings and the Gulf of Mexico area with more moderate (500 cm^{-3}) and "cleaner" (200 cm^{-3}) CCN values, respectively. All runs focused on effects of urban CCN enhancement and therefore, giant CCN concentrations were homogeneously initialized in an identical manner for all runs.

3.3 Instability and indirect aerosol effects

A third series of numerical experiments consisted of a rather large number (over 100) of multi-grid simulations and varied both the strength of aerosol pollution and convective instability.

The initial temperature field corresponding to the case study was modified to consider environments with different convective instability. We added or subtracted constant values to the temperature vertical profiles of finest grid (grid 3) approximately between cloud base and 10000 m in such a way that the convective available potential energy (CAPE) varied between 400 and 1600 Jkg^{-1} . In most cases CAPE was varied at 100 Jkg^{-1} intervals, however, we considered 50 Jkg^{-1} intervals for some urban aerosol intensities. Those temperature differences were smoothed out within grid 2 to avoid numerical discontinuities.

City CCN sources were also considered by nudging these high concentrations at the first model level above the ground multiplied by the sub-grid urban fraction of the corresponding grid cell (derived from the NLCD data). We considered nudged values of 500, 1000, 1500, 2000, 2500, 3000, 3500, and 4000 cm^{-3} , as well as a city with no aerosol sources.

3.4 Direct aerosol effects

The last series of simulations considered both indirect and direct effects. The experimental design was identical to that of 3.2; however, only the 2001 NLCD satellite data was used to initialize the urban grid cells and sub-grid fractions. A set of new simulations took into account only direct effects while the other considered both indirect and indirect.

4. SUMMARY OF RESULTS

4.1 Validation

We evaluated the model performance in reproducing some general characteristics of the 24 August 2000 case study. The simulated precipitation rates averaged over grid 3 and accumulated values are compared to those derived from radar data in Fig 2. The accumulated values simulated using 2001 satellite data and 2000 cm^{-3} CCN sources were comparable although slightly higher than those observed (Figs. 2. a and c, respectively). The simulated temporal evolution and the location of the most intense cells are in good agreement with the radar-derived data.

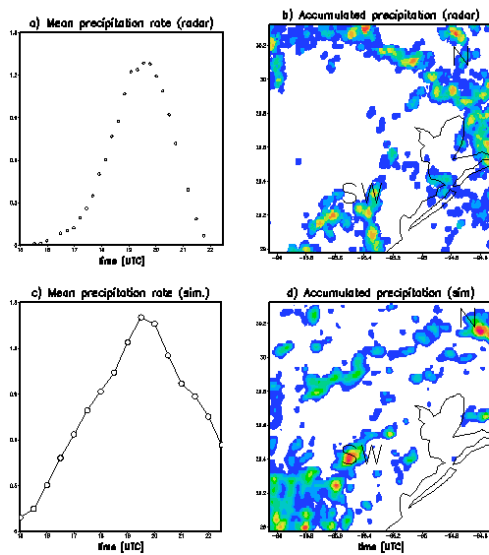


Figure 2. Evolution of the radar-derived and simulated precipitation rates averaged over grid 3 for the run using 2001 satellite data and 2000 cm^{-3} CCN sources (a and c). Ordinates represent precipitation rate in mmh^{-1} and abscissas, the simulation the UTC time. Shaded areas are the radar-derived and simulated accumulated precipitation expressed in mm (b and d, respectively).

4.2 Urban size runs

The intensity of the sea-breeze (~SE) increased monotonically for larger urban areas. The intensity of the mass flux averaged over the lowest km is compared in figure 3 for 1992, 2001, and 2006 runs. These plots correspond to a time one hour before the most intense activity occurred (~ 18:30Z).

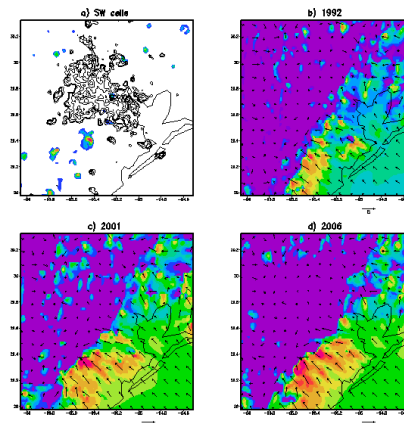


Figure 3. The shaded areas in panels b, c, and d show the southeast flux for 1992, 2001, and 2006 land use, respectively. These fluxes were computed at a simulation time that corresponds to one hour prior to the most intense convective activity (18:30 UTC). 1 m s^{-1} intervals.

Varying the city size exhibited a dramatic impact on precipitation. Figure 4 compares the evolution integral volume of precipitation simulated for different scenarios: NO CITY, and considering 1992, 2001, and 2006 land-use satellite data. This figure shows differences (up to 26%) in the simulated precipitation volume with respect to the NO CITY run.

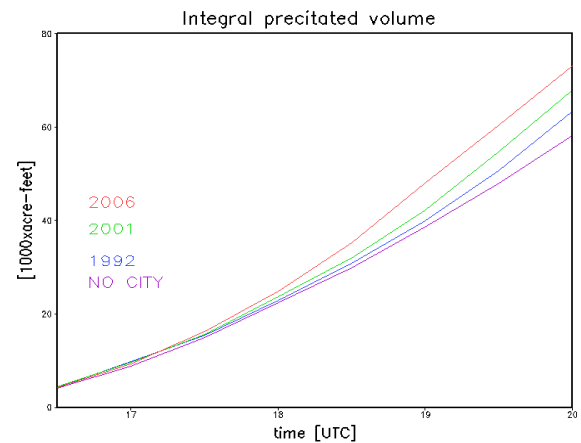


Figure 4. Comparison of the precipitated volume simulated for different city sizes (2000 cm^{-3} CCN sources).

This precipitation enhancement is more linked to an important increase in the area of the storm than to an increase in the intensity of the convective

cells. This is evident in Figure 5 that compares the maximum liquid water paths (LWPs) and the areas with precipitation.

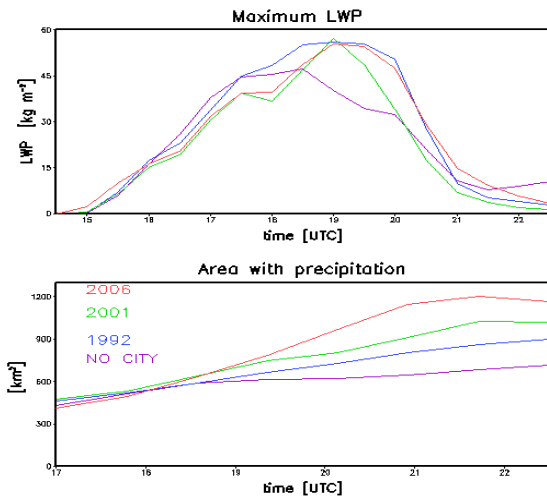


Figure 5. Comparison of the evolution of simulated LWP maxima and area with precipitation.

Moreover, areas with updrafts covered a larger area for “larger cities” but updraft maxima did not show a regular behavior (not shown). Conversely, downdrafts tended to be stronger for larger urban areas (not shown). The latter result could be linked to the higher number of convective cores that develop.

4.3 Aerosol indirect sensitivity runs

The vertical profiles of updraft intensity and mixing ratios of pristine ice, aggregates, rain, and the large precipitating ice-phase species (hail and graupel) are compared in Fig. 6 for runs considering a clean city, and the 2001 land use with different aerosol source intensities. Vertical profiles in Figs. 6a, b, c, and d correspond to the time and the location at which, for each run, the maximum updraft is attained. Updraft maxima are higher for the “polluted cities” and they occur at a higher altitude compared to that of the clean city. The mixing ratio of pristine ice monotonically increases and the corresponding diameters monotonically decrease when using more intense urban sources (Figs. 6b and c). With higher CCN concentrations, liquid drop coalescence and riming is suppressed and therefore more small droplets reach supercooled levels and lightly-rimed ice crystals are transported to the top of the cloud. In addition, more numerous and smaller liquid particles reach the layer with temperatures between -30 and -40° and become pristine ice

crystal via homogeneous nucleation of cloud droplets and haze particles. The vertical profiles of the large precipitation particles (rain and hail+graupel) were averaged over a period of 30 min after the maximum updraft was attained (Figs. 6e and f). This was done to take into account the expected delay in the effects on these hydrometeors. The mixing ratios of rain and large ice-phase hydrometeors (hail + graupel) did *not* exhibit a monotonic behavior. The highest mixing ratio was simulated for the run with 1000 cm^{-3} CCN sources and then it decreased when considering more polluted cities. As we mentioned above, enhancing CCN concentrations leads to larger numbers of smaller drops being able to reach supercooled levels, freeze, and potentially enhance precipitation. However, when CCN concentrations are further enhanced, riming of ice particles become less efficient. This opposing effect leads to a greater fraction of condensate transported out into storm anvils and a reduction in the precipitation efficiency. As seen in Fig. 6 d, the mixing ratio of aggregates behaves similarly to that of rain. It first increases from the clean city run to the run with 1000 cm^{-3} CCN urban sources and then decreases when considering more intense urban sources, with values below those in the clean city for the runs with 2000 and 4000 cm^{-3} CCN sources. The first increase (from the clean city run to the run with 1000 cm^{-3} sources) may be explained by the enhanced availability of supercooled liquid water. When further increasing CCN concentrations, both pristine ice crystals and cloud droplets are smaller, the collision efficiencies are lower and riming is suppressed.

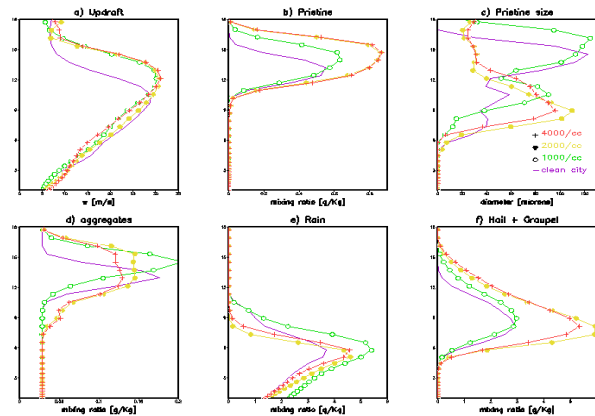


Figure 6. Vertical profiles simulated for each CCN source intensity and the clean city run (2001 land use). Updrafts are expressed in ms^{-1} , mixing ratios in gkg^{-1} , and ice crystal size in microns. Ordinates are the altitude in km.

We also compared the peak conversion rates to aggregates simulated for these runs (not shown). For the numerical experiment with the lowest pollution level, this peak conversion rate was 23% above that simulated for the clean city run. When increasing the CCN source intensity from 1000 to 2000 cm^{-3} , this peak rate decreased 33%, and decreased 14% when increasing this intensity from 2000 to 4000 cm^{-3} .

All comparisons made in Fig. 6 correspond to runs that used 2001 satellite data, although the main results remain valid for 1992 and 2006 cities.

4.4 Aerosol effects and instability

The variation of the altitude at which the maximum updraft is attained (downwind region) is shown Fig. 7. Shaded areas denote differences with respect to the altitude that corresponds to the run that uses the environmental conditions of case study and a clean city. For each CAPE value, the pollution level that corresponds to the highest altitude difference is indicated by an open triangle. For all runs, the peak updrafts were attained at higher altitudes (respect to clean city). It takes higher CCN concentration for more unstable environments. As expected, the largest impact corresponds to low instability runs.

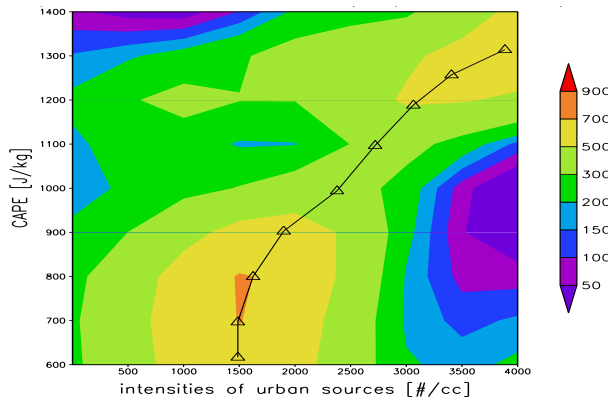


Figure 7. Altitudes at which the maximum updraft is attained (m, respect to that of a clean city).

The maximum precipitation accumulations over the downwind area are given in Fig. 8. For each CAPE value, the pollution level for which the highest accumulation was simulated is indicated by an open circle. Simulated accumulated maxima exhibited differences up to 12%. For each level of instability, when urban CCN concentrations increase, the maximum accumulated precipitation downwind first increases, and then decreases. The “optimal” CCN concentration is higher for runs with higher instability.

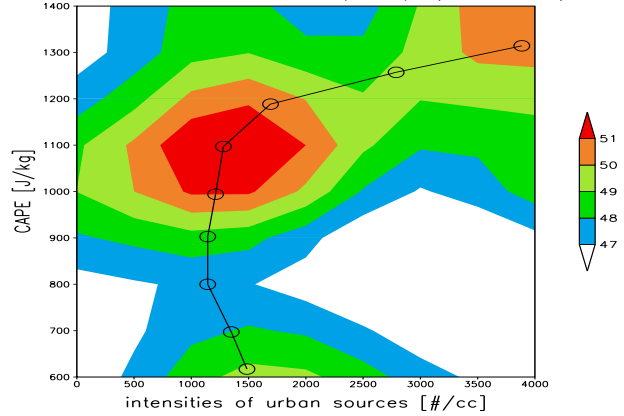


Figure 8. Maximum accumulated precipitation downwind of the city (mm).

We computed the ratio between the total water mass precipitated over the downwind area and the temporal integration of the upward vapor flux at approximately cloud base levels. Those ratios represent precipitation efficiencies and are given in Fig 9 for all runs. It must be noted that the peak values (denoted by an **E**) occur for higher aerosol concentrations for runs with higher CAPE and the ratios decrease with more intense urban aerosol sources.

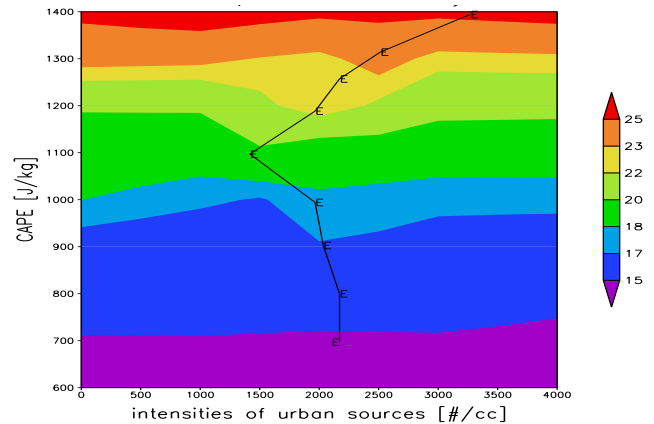


Figure 9. Estimation of the precipitation efficiency (%) for downwind cells.

Figure 10 gives the mass weighted diameters of the supercooled droplets in convective cells downwind of the city. The curves corresponding to the maxima of precipitation accumulation (open circles) and the integral SC water mass (symbol **M**) have been superimposed to this figure. Both curves are contained in the region where SC droplet sizes are between 4.5 to 5 μm .

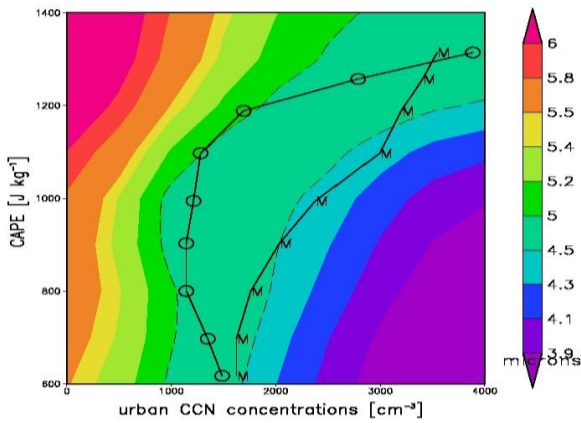


Figure 10. Diameters of supercooled droplets.

Comparing Figs 9 and 10, it can be seen that the decrease in precipitation efficiency (after each corresponding peak value) is more likely to be linked to a change in microstructure of the convective cells change than to a dynamic effect.

4.5 Radiative effects of urban pollution

All runs considering the radiative effect of the urban aerosols showed a slight decrease in surface temperatures. The temperature vertical profiles averaged over the area cover by the aerosol plume are compared in Fig. 11 for the hour previous to the start the intense convective activity.

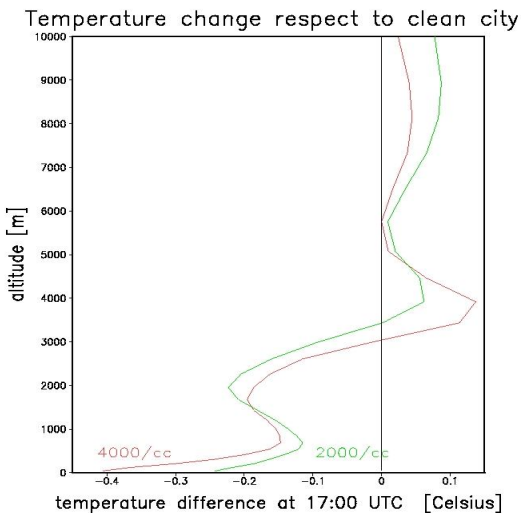


Figure 11. Temperature difference produced by two levels of pollution (with respect to the corresponding runs that do not consider aerosol radiative effects).

This low-level temperature decrease produces a small although not negligible reduction in the intensity of the sea-breeze (Fig 12).

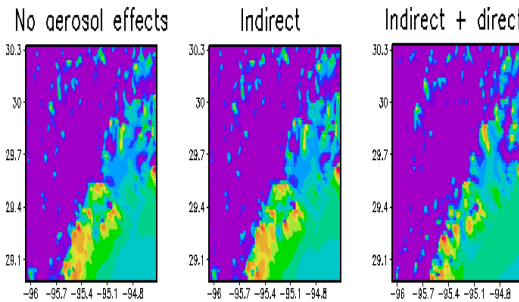


Figure 12. The shaded areas compare the southeast flux averaged over lowest 1000 m at a simulation time that corresponds to one hour prior to the most intense convective activity (18:30 UTC). 1 m s⁻¹ intervals.

The radiative effects oppose indirect effects although they are less important as it can be seen in Figure 13. This figure compares the time evolution of the integral precipitated volume for run considering no aerosol effects, indirect or direct effect only, and both combined.

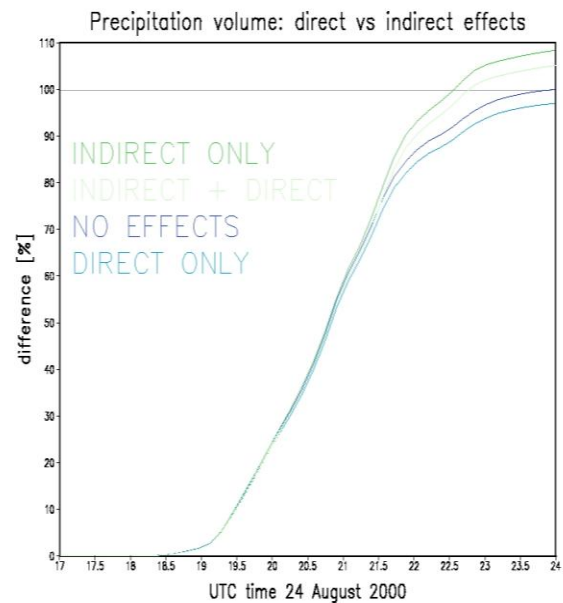


Figure 13. Evolution of the integral volume of precipitation (percent normalized by the total corresponding to the no aerosol effects run).

5. CONCLUSIONS

We examined the effect of Houston's urban growth on convection/precipitation isolating the urban pollution aerosol direct and indirect effects and land-use change impact.

In summary, when considering "larger cities" we simulated:

- Higher precipitation rates over the finest grid, the NO CITY run exhibits a maximum much later.
- The precipitation rates and accumulated values over urban cells showed lower but positive differences.
 - Increased intensity of the sea breeze.
 - Total volume of precipitation (finest grid) increased monotonically 9, 11, and 26% (over NOCITY) for 1992, 2001, and 2006, respectively,
 - LWPs and updrafts maxima did not change significantly,
 - Conversely, the integral value of condensate and maximum downdrafts increased. The latter result is linked to the larger area coverage of the storm.

While "more polluted cities" resulted in:

- Positive differences in LWC maxima and differences up to 9% for supercooled water mass.
- Small differences in the total precipitated volume for both the entire domain and the city.
- However, there is a significant increase in the accumulated precipitation linked to the most intense cells downwind of the city.
- Non-monotonic impact on accumulated precipitation maxima of the cells.

When considering more or less unstable environments:

- Again, a non monotonic response of accumulated precipitation maxima (independent of the value of CAPE).
 - It first increases from the clean city run to a certain level of particulate pollution and then decreases when considering more intense urban sources.
 - Updraft maxima altitude, integral mass of supercooled liquid water, and precipitation efficiency also exhibited a non-monotonic behavior.
 - Further enhancing urban aerosol concentrations reduces the efficiencies of riming

processes, responsible of the rapid transfer of the SC liquid water to the ice phase and and larger amounts of condensate were transported upwards into the storm anvil.

- For more unstable environments, the peak values of these quantities corresponded to higher levels of pollution. Larger overall upward fluxes and therefore more intense CCN sources are required to produce equivalent micro and macrophysical effects.
- The increase of the particulate pollution is more likely to selectively enhance precipitation of convective events characterized by higher instability.

And, for radiative effects of urban pollution:

- Surface cooling produces a small although non-negligible reduction of convective instability, intensity of the sea-breeze, and precipitation.
- Results suggest that the radiative effect is less important than the indirect effect for sea-breeze-induced storms over Houston.

6. ACKNOWLEDGEMENTS

The authors want to thank NOAA for financial support (NA07OAR4310281).

7. REFERENCES

- Carrió, G. G., Cotton, W. R., Cheng W. Y. Y., 2010: Urban growth and aerosol effects on convection over Houston. Part I: the August 2000 case. *Atmos. Res.*, **96**, 560-574.
- Carrió, G. G. and W. R. Cotton, 2011: Urban growth and aerosol effects on convection over Houston. Part II: Dependence of aerosol effects on instability submitted to *Atmos. Res.*.
- Cotton, W.R., R.A. Pielke Sr., R.L. Walko, G.E. Liston, C.J. Tremback, H. Jiang, R.L. McAnelly, J.Y. Harrington, M.E. Nicholls, G.G. Carrió, and J.P. McFadden, 2003: RAMS 2001: Current status and future directions. *Meteor. Atmos. Phys.*, **82**, 5-29.
- Lance, S., and coauthors, 2009: CCN Activity, Closure and Droplet Growth Kinetics of Houston Aerosol During the Gulf of Mexico Atmospheric Composition and Climate Study (GoMACCS), *J.Geoph.Res.*, **114**, D00F15, doi:10.1029/2008JD011699.
- Saleeby, S. M., and W.R. Cotton, 2008: A Binned Approach to Cloud-Droplet Riming Implemented in a Bulk Microphysics Model. *J. Appl. Meteo*, **47**, 694-703.
- Saleeby, S. M., and W.R. Cotton, 2004: A large-droplet model and prognostic number concentration of cloud droplets in the RAMS@CSU model. Part I: Module descriptions and Supercell test simulations. *J. Appl. Meteo*, **43**, 182-195.